The Significance of Melt Practice on Fatigue Properties of Superelastic NiTi Fine Diameter Wire

M. M. Patel, D. L. Plumley, R. J. Bouthot
Fort Wayne Metals Research Products Corporation,9609 Indianapolis Road, Fort Wayne, Indiana 46809, USA

J. L. Proft
Metallurgical Solutions,203 Redwood Shores Parkway, Suite 230, Redwood City, California 94065, USA

Abstract

In continuation of a previous comparison of the influence of melt practice and strain amplitude on Ni 56wt%-Ti 0.267 mm wire, this investigation explores the fatigue properties at 0.127 mm of the same melt lots. By employing the same rotary beam fatigue testing, material with equivalent thermo-mechanical processing to achieve like superelastic properties is compared. With known statistically detectable variations in carbon level and inclusion content, testing again focused on determining if there is a difference in rotary beam fatigue performance. In contrast to the results of the previous study, there is evidence of a difference in performance for the smaller diameter wire among melt sources. Possible explanations for this difference and its significance are discussed.

Introduction

As mentioned by Reinoehl et al, carbon content in the ingot chemical composition is noted as the primary difference among the two raw material suppliers compared in this study [1]. The carbon content in the redraw wire stock from Supplier A was 0.0033 wt%; on the other hand, Supplier B offered material with a 0.0365 wt% of carbon. Through this previous work it was shown that materials with statistically detectable differences in carbon level, inclusion content, plateau strengths, and Active Austenitic Finish values demonstrated equivalent fatigue behavior at 0.267 mm. Table 1 compares the ingot properties of both alloys. Ingot transformation temperature range (TTR) values listed are vendor certified data.

Table 1: Ingot Characteristics

	Supply A	Supply B
TTR	M_s = - 34°C; M_p = - 37°C; M_f = - 53°C A_s = - 25°C; A_p = - 14°C; A_f = - 7°C	M_s = - 40°C; M_p = - 44°C; M_f = - 54°C A_s = - 24°C; A_p = - 17°C; A_f = - 14°C

An inclusion analysis was performed on raw material received from Suppliers A and B. Results from the longitudinal cross sections are found in Table 2.

Table 2: Longitudinal Inclusion Analysis ~2.16 mm

	Supply A	Supply B
Total Inclusions	17180	33700
> 2 µm Inclusions	1205	359
Largest Defect Size	10 µm	5 µm
Stringer Length (Average)	3451 µm	384 µm

After the shape-setting or straight annealing processes, final Active A_f temperatures were 9°C for Supplier A and 14°C for Supplier B. The implication of this thermal property and its influence on fatigue life for a particular environment was explored through rotary beam fatigue testing (RBT) [2].

Through continued thermomechanical processing, including cold drawing, inter-pass annealing, and equivalent training heat treatments, a comparable medical grade Nitinol fine wire was fabricated. The current study focuses on 0.127 mm Nitinol (Ni 55.8wt%-Ti; Ti 49.2at%, Ni 50.8at%) wires in the zero mean strain condition. The final Active A_f temperatures are now 13°C for Supplier A and 21°C for Supplier B. As the wires rotate, the outer wire surfaces at the apex of the bend are exposed to a cyclic stress reversal of tension and compression states [3]. As device design engineers tackle material

9609 Indianapolis Road, Fort Wayne, IN 46809 - Tel: 260.747.4154 - Web: http://www.fwmetals.com
Presented at The International Conference on Shape Memory and Superelastic Technologies (SMST) Pacific Grove, CA May 2006

selection issues, importance must be placed on the interrelationships between structural and property characteristics. The goal of this testing approach is to offer those engineers, working with fine diameter Nitinol wires, additional information on the sensitivity of fatigue performance to chemical composition, structural changes, mechanical properties, thermal properties, and testing environments.

In the comparison study completed in 2000, the differences in the test materials' Active A_f were not considered a detrimental factor while testing. To circumvent a similar oversight, in the current research the final thermal properties of the Niti wire, while in the shape-set condition were considered when determining the RBT temperature. Reinoehl found that through testing at room temperature (nominally 23°C), no statistical difference in fatigue cycles completed were detected between the two alloy suppliers [1]. The strain-life (ε-N_f) curve associated with this finding is shown in Fig. 1.

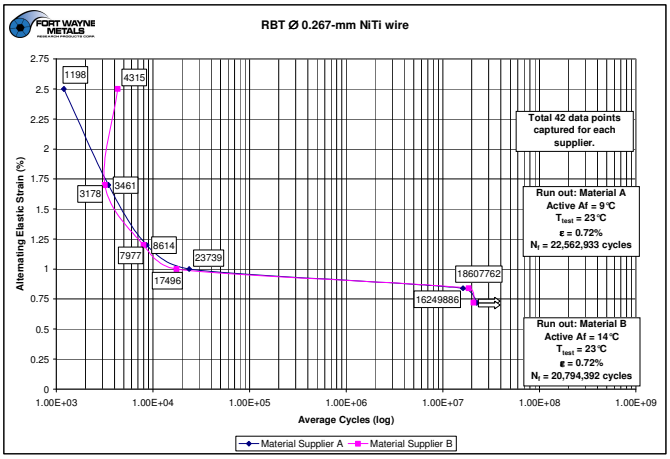

Figure 1: RBT Comparison data at 0.267-mm

Materials and Methods

The Nitinol round wires, taken from the same supplier ingots as Reinoehl utilized, were cold worked from 2.16 mm to 0.267 mm, and then to 0.127 mm with nominally 45% reduction in area on the final diamond drawing die sequence [1]. The materials were then straight annealed resulting in Active A_f values at 13°C and 21°C for suppliers A and B, respectively. The straight annealing process for these materials were completed with the same inert atmosphere, dwell time, temperature, and tension.

As well documented, the dependence of stress and strain with temperature change in Nitinol materials follows the Clausius-Clapeyron relationship [4]. Tensile testing and RBT testing were conducted at nominally 10°C above the final Active A_f transformation temperature ($\Delta T = \{|T_{test}\text{-Active } A_f|\} = 10°C$); these temperatures were chosen to create a baseline for material stress conditions of final medical-grade wires [2]. Tensile properties were evaluated in a temperature-controlled environmental chamber at the desired temperatures. A Positool Rotary Beam U-Bend Wire Spin Fatigue Tester (Model #10-040) was employed to evaluate the fatigue performance of the NiTiNOL round wires [5]. RBT was executed in a circulating, temperature-controlled water bath. The following strain levels (%) were tested: 0.80, 0.90, 1.00, 1.50, 2.00. The 2.50% strain level was not tested due to equipment limitations. Seven round wire specimens were tested for each strain level. Test completion was based on either wire fracture or by reaching a run out criteria for each strain level. Test protocol allowed the wire to be rotated up to 100 million alternating cycles. The material was cycled at a constant frequency of 3,600 revolutions per minute (RPM) [3]. Figure 2 plots the ε-N_f curve based on the aforementioned testing conditions.

Experimental Results

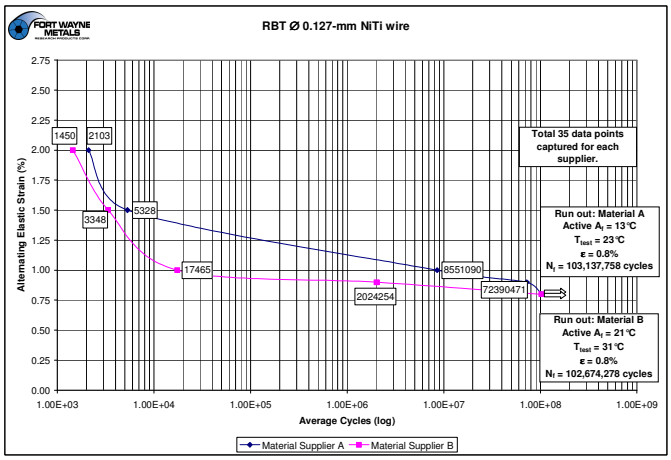

Figure 2: RBT Comparison data at 0.127-mm

By utilizing Scanning Electron Microscopy equipped with the Backscattered Electron Imaging (SEM-BEI) fracture surfaces were evaluated for morphology and the Energy Dispersive X-ray Spectroscopy (EDS) function was employed to compare chemical composition. Samples evaluated were the minimum and maximum cycles completed for each strain level. Similar to what was found previously, the fracture surfaces were

9609 Indianapolis Road, Fort Wayne, IN 46809 - Tel: 260.747.4154 - Web: http://www.fwmetals.com
Presented at The International Conference on Shape Memory and Superelastic Technologies (SMST) Pacific Grove, CA May 2006

typical of fatigue fracture mechanisms and partly due to ductile fracture mechanism for the remainder of the cross section [1, 2]. Radial markings on the fracture surfaces indicate a single initiation site at or near the surface of the wire for all fractures; other surfaces had radial markings on the fracture surfaces indicated by multiple crack initiation sites within a small area on the surface of each sample.

For Supplier A, the smallest inclusion at 0.127 mm discovered through all RBT fractured specimens are shown in Figs. 3a and 3b. The images exhibit radial markings and the texture of a fracture surface with a single initiation site. The defect is at or near the wire surface. The fracture origin area was oriented at an oblique angle to the remainder of the transverse fracture. The fracture area comprised 46% of the wire cross section. The nonmetallic inclusion had an angular shape and was about 1.2 µm in the transverse dimension. The EDS analysis in Fig. 4 shows the composition of the inclusion to be N, Ti, and O.

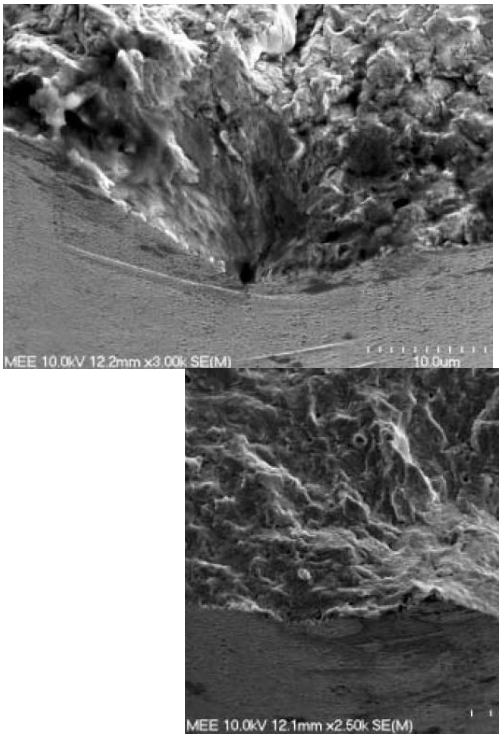

Figures 3a and 3b: Mating Fracture Sides A & B.

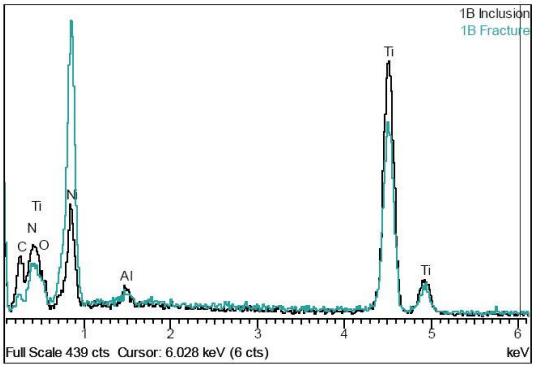

Figure 4: EDS spectra of the smallest inclusion matter for Supplier A.

The smallest inclusion found in the wires tested for Supplier B (Fig. 5) had radial markings and surface texture for the fracture with three independent crack initiation sites around the wire surface. The fracture area comprised 35% of the wire cross section. The crack from one of the origin sites became the primary fracture, coalescing with the crack from the second origin. One of the secondary initiation sites never linked with the primary fatigue crack. An inclusion was observed near the surface of the wire at the primary area with an angular shape and was 3.7 µm across. A few small, secondary cracks were observed on the wire surface near the fracture. The microscopic features in the fatigue area consisted of distinct striations; the final fracture area had a dimpled morphology. EDS spectra, Fig. 6, for this inclusion was comprised of Ti, Ni, O, C, and N.

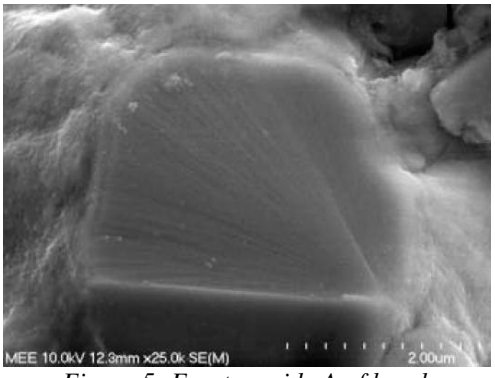

Figure 5: Fracture side A of break

9609 Indianapolis Road, Fort Wayne, IN 46809 - Tel: 260.747.4154 - Web: http://www.fwmetals.com
Presented at The International Conference on Shape Memory and Superelastic Technologies (SMST) Pacific Grove, CA May 2006

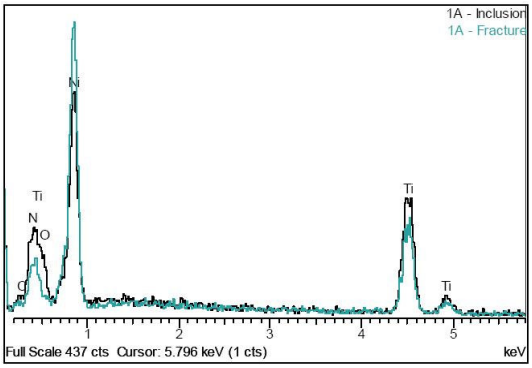

Figure 6: EDS spectra of the smallest inclusion matter for Supplier B.

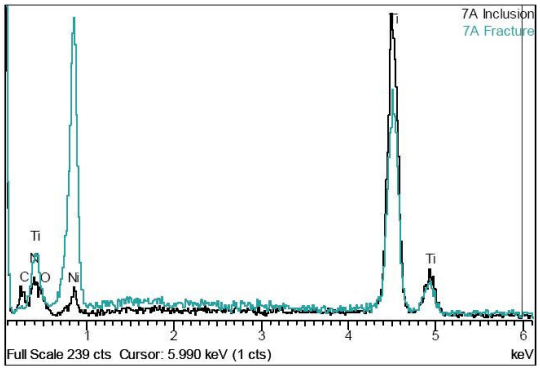

Figure 8: EDS spectra of the largest inclusion matter for Supplier A.

The largest inclusion found in material at 0.127 mm for Supplier A is imaged in Figs. 7a and 7b. has radial markings and texture of the fracture surface indicating a single initiation site at or near the wire surface. The fatigue fracture area comprised about 61% of the wire cross section. The nonmetallic inclusion at the wire surface at the initiation site had an angular shape and was about 3.5 µm across. Figure 8 displays the chemical traits of this inclusion to be mainly N, Ti, C, and O.

In material produced from Supplier B, wire ends had radial markings and the texture of the fracture surface indicating a single initiation site at or near the wire surface. The fatigue fracture area comprised about 50% of the wire cross section. A nonmetallic inclusion was observed at the wire surface fractures initiation site. The inclusion had an angular shape and was about 4.4 µm across, shown in Figs. 9a and 9b. EDS in Fig. 10 confirmed that once again Ti, Ni, O, C, and N elements are present.

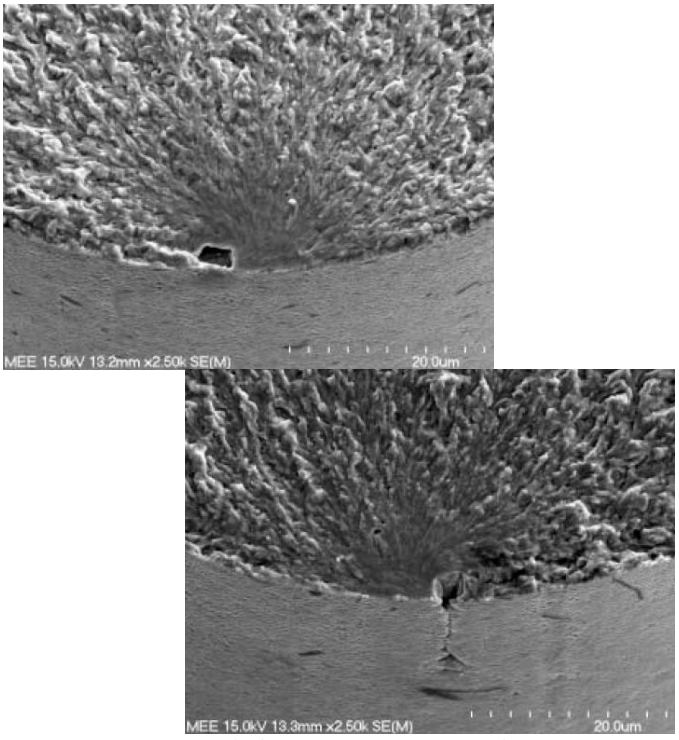

Figures 7a and 7b: Mating Fracture Sides A & B.

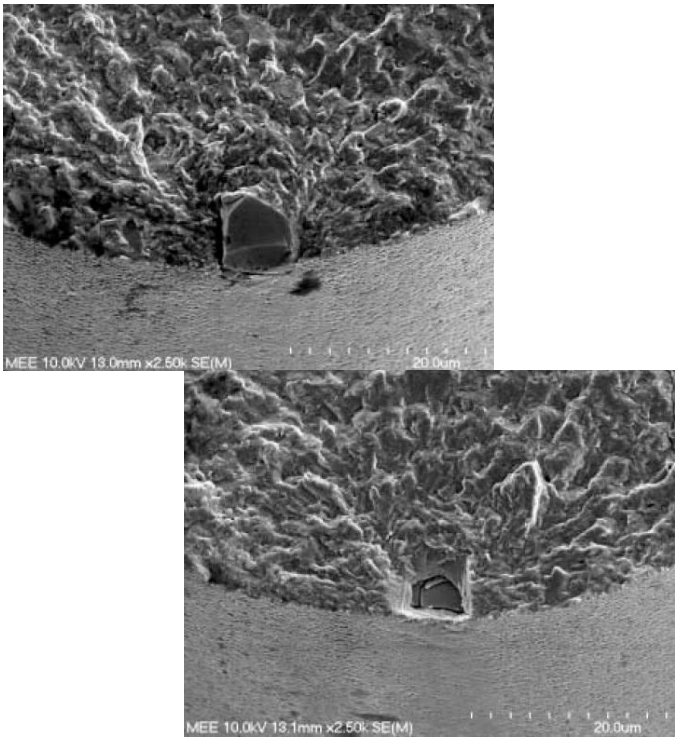

Figures 9a and 9b: Mating Fracture Sides A & B.

9609 Indianapolis Road, Fort Wayne, IN 46809 - Tel: 260.747.4154 - Web: http://www.fwmetals.com
Presented at The International Conference on Shape Memory and Superelastic Technologies (SMST) Pacific Grove, CA May 2006

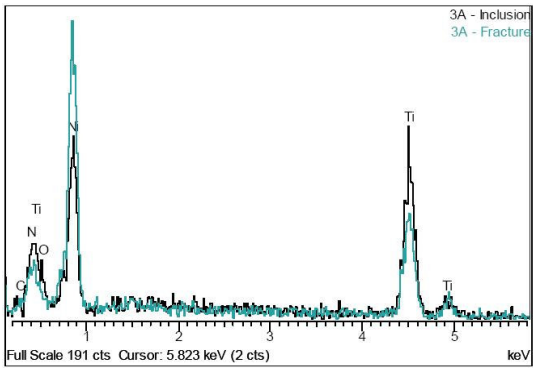

Figure 10: EDS spectra of the largest inclusion matter for Supplier B.

Table 3 displays the mechanical and thermal properties recorded for the 0.267 mm wire.

Table 3: 0.267 mm Wire Mechanical Properties tested at 23°C [1]

Material Characteristic (Mean)	Supply A	Supply B
Ultimate Tensile	1475.1 N/mm^2	1496.9 N/ mm^2
Elongation to Failure	14.2%	14.2%
Loading Plateau Strength	628.9 N/mm^2	618.9 N/mm^2
Unloading Plateau Strength	265.7 N/mm^2	243.0 N/mm^2
Active A_f	9.3°C	13.6°C

For comparison, Table 4 compares the same properties for the 0.127 mm wire.

Table 4: 0.127 mm Wire Mechanical Properties tested at 10°C above Active A_f

Material Characteristic (Mean)	Supply A	Supply B
Ultimate Tensile	1543.3 N/mm^2	1551.3 N/mm^2
Elongation to Failure	14.7%	14.2%
Loading Plateau Strength	525.7 N/mm^2	566.0 N/mm^2
Unloading Plateau Strength	208.0 N/mm^2	275.2 N/mm^2
Active A_f	13.4°C	21.1°C

Discussion

Few samples from Supplier A have fractures without inclusions present. Inclusions found in wire made from Supplier A have a lower net Ni percentage than those in Supplier B when analyzed using EDS. All inclusions found in material from Supplier B had high concentrations of nickel. Some brittle, ceramic inclusions divided and could be located on both sides of the mating surfaces. In the rare instances where there was an absence of inclusions in the fracture area, small secondary cracks were identified on the wire break surface. When an angular pit was observed, but no inclusions were found, an inclusion may have once resided in that location, but had fallen out after fracture. Previous studies have found similar defects [1, 2]. It is hypothesized that nickel-rich compounds found in samples from Supplier B, may lead to the elevated final TTR of the final fine wire product. In addition, the nickel atoms in the Ni-Ti metal matrix were bonded to trace elements forming extrinsic defects.

Summary and Conclusion

The aim was to decipher whether a trend of fatigue life is achievable through varying the carbon content and possibly the hot and cold working upstream, while maintaining similar processing downstream. Both suppliers' materials were processed with constant parameters. Annealing dwell time, temperatures, and atmosphere were identical. Furthermore, drawing speeds and cold work reductions were matched as well.

1.) As concluded from Tables 4 and 5, the spread in Active A_f between suppliers increased at the finer wire diameter; moreover, both Active A_f temperatures also increased. Figure 11 is a graphical representation of this phenomenon. It is possible a portion of the TTR shift may also be attributed to residual cold work in the wire.

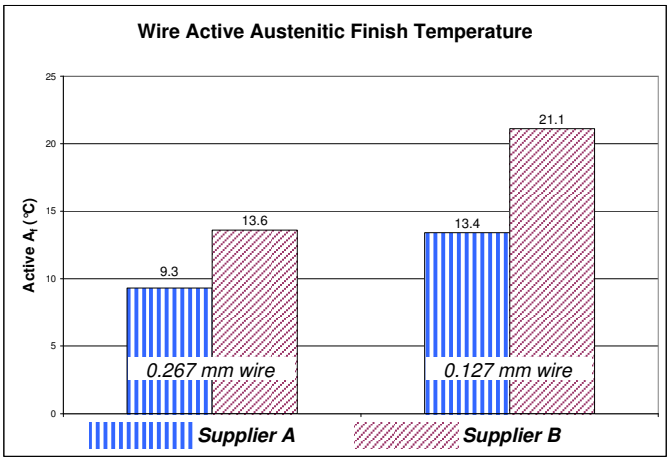

Figure 11: Active A_f values at 0.267 mm and 0.127 mm.

2.) As shown in Fig. 12, a change was also observed regarding mechanical properties. An inverse relationship exists between suppliers' materials. The Supplier B material exhibited higher plateau strengths at 0.127 mm diameter whereas Supplier A was greater at 0.267 mm.

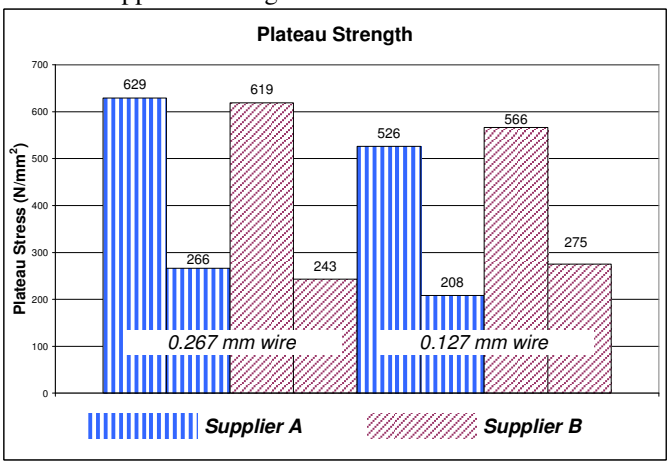

Figure 12: Plateau Strengths at 0.267 mm and 0.127 mm.

3.) In contrast to previous findings by Reinhoel, a significant difference was observed at the intermediate strain values of 0.9% and 1.0% [1]. Inclusion sizes are more critical to fatigue fractures at finer diameter of round wires. These defects consume much more of the cross section in the smaller fine wire.

4.) The raw materials were acquired in November and December of 1999 for Suppliers A and B, respectively. A greater number of recently melted heats from each supplier should be compared.

Ideas for Future Research

1.) Accurately determine the Stress-Induced Martensite strain level; then focus testing above and below this value

2.) Determine role of grain structure of the solidified ingot and implications on fatigue at fine wire

3.) Explore influence of hot rolling of the Nitinol rod stock

4.) Track inclusion morphology throughout each major processing phase

5.) Determine the affect of inclusion chemistry on the final product

6.) Design experiments of non-zero mean strain testing for the same materials tested at zero mean

Acknowledgements

The authors would like commend those who assisted in the wire drawing and laboratory testing of the research materials used in this study. In addition, a special thank you is being extended to the team at MEE (Materials Evaluation and Engineering) for the fracture surface analysis of the specimens.

References

[1] Reinoehl, M. et al., in *SMST-2000: Proceedings of the International Conference on Shape Memory and Superelastic Technologies*, eds. S.M. Russell and A.R. Pelton, Pacific Grove, California: International Organization on SMST, 2001, pp. 397-403.

[2] Patel, M. et al. "The Effects of Varying Active A_f Temperatures on the Fatigue Properties of Nitinol Wire". Presented at the ASM MPMD Conference, Boston, MA Nov, 2005.

[3] Patel, M. et al. "Characterizing Fatigue and Fracture Response of Medical Grade Nickel-Titanium Alloys by Rotary Beam Testing". Presented at the ASTM Seminar, Dallas, TX, Nov, 2005.

[4] Otsuka, K. and Wayman, C.M., *Shape Memory Materials*, Cambridge University Press, New York, 1998, pp. 25.

[5] Operating manual, Positool, Rotary Beam U-Bend Wire Spin Fatigue Tester Model 10-040.